Asian Journal of Chemistry; Vol. 35, No. 11 (2023), 2815-2821

ASIAN JOURNAL OF CHEMISTRY

https://doi.org/10.14233/ajchem.2023.30256

Synthesis, Characterization, Antimicrobial and Cytotoxic Investigations of Some Transition Metal(II) Complexes with Tridentate Schiff Base Derived from Pyrrolopyrimidine

ABHAY BAGUL[1,2], DIGAMBER GAIKWAD[1,*], YOGESH PATIL[2] and NILESH BHUSARI[3]

[1]Department of Forensic Chemistry, Government Institute of Forensic Sciences, Aurangabad-431004, India
[2]Department of Chemistry, Vasantrao Naik Mahavidhyalaya, Aurangabad-431003, India
[3]Department of Chemistry, Maulana Azad College of Arts, Science and Commerce, Aurangabad-431004, India

*Corresponding author: E-mail: gaikwad.dd.dg@gmail.com

Received: 10 September 2023; *Accepted*: 23 October 2023; *Published online*: 31 October 2023; AJC-21440

A Schiff base pyrrolopyrimidine-hydrazide-*m*-chlorobenzaldehyde (HPPH*m*CB) was synthesized *via* condensation reaction between a pyrrolopyrimidinehydrazide and 3-chlorobenzaldehyde and its transition metal(II) complexes complexes followed by the characterization and electrochemical analysis. The magnetic susceptibility, electrolytic conductivity, elemental analysis, FT-IR, electronic absorption, ESR and PMR spectra were employed to elucidate the structural properties. The Schiff base HPPH*m*CB ligand acts as a tridentate N,N,N donor and produces complexes of type $[M(PPHmCB)_2]$, which exhibit a square planar geometry for Pd(II) complex, tetrahedral for Hg(II), Cd(II) and Zn(II) complexes and octahedral geometry for Mn(II), Cu(II), Fe(II), Co(II) and Ni(II) complexes. The minimum inhibitory concentration (MIC) approach was used to screen the *in vitro* antibacterial and antifungal activities of synthesized Schiff base HPPH*m*CB ligand and its metal(II) complexes. The results showed that the significant microbial activities by both ligand and its transition metal(II) complexes. Moreover, *in vitro* cytotoxicity properties of Schiff base HPPH*m*CB ligand and its metal(II) complexes were also investigated against *Artemia salina* using the brine shrimp bioassay.

Keywords: Schiff base, Cytotoxicity properties, Pyrrolopyrimidine, Microbial activities, Transition metal(II) complexes.

INTRODUCTION

Majority of the coordined metal complexes incorporate various kind of Schiff bases as ligands [1,2]. These conveniently available ligands provide functional variety and a range of coordination numbers. This phenomenon is possible due to their one-of-a-kind chemical structures and the components used in their production. Furthermore, the interesting properties of homo- and hetero-polynuclear complexes can be influenced by the O, N and S donor atoms in Schiff base-derived ligands, the types of those donor atoms and the relative locations of those donor atoms concerning the central metallic atom [3-6]. Due to several benefits, the researchers in various fields like separation science, transport, bioinorganic chemistry, analytical chemistry, encapsulation, catalysis and magnetochemistry have been inspired to synthesize metal complexes [7-11]. Because of the high binding constants that they display for a variety of *d*- and *f*-block metals [12] have led to a surge in interest in macrocyclic Schiff base ligands, which are both simple to synthesize and versatile enough to act as multidentate ligands. Several chromatographic techniques and optical and electrochemical sensors use Schiff base ligands to enable more selective and sensitive detection [13-15].

Metal ion complexes with pyrimidine derivatives have attracted attention [16] due to their biological activity against viruses, malaria, bacteria and tumors. In addition, numerous luminescent heterocyclic metal complex drug preparations with promising properties have also been reported in the literature. Complexes with similar structures may have been used in materials research as precursors for the optical materials [17]. The Schiff base ligand pyrrolopyrimidinehydrazide-3-chlorobenzaldehyde (HPPH*m*CB) and its transition metal(II) complexes have been synthesized and characterized in this work. To characterize the HPPH*m*CB ligand and its metal(II) complexes, the instrumental techniques such as FTIR, UV-Vis, magnetic moments and electron spin resonance (ESR) were used for characterization.

EXPERIMENTAL

All the metal(II) chloride salts and solvents *viz*. DMF, DMSO, methanol, ethanol, chloroform, nitrobenzene, butanol, 3-chlorobenzaldehyde, (99%, HPLC grade, spectrophotometric grade) were purchased from S.D. fine and Merck, respectively and used as received.

To characterize the Schiff base HPPH*m*CB ligand and its metal(II) complexes, experimental techniques such as FT(IR), electronic absorption spectra, magnetic moments and ESR were performed. Using Brucker-400 a spectrometer, the spectra of ^{1}H NMR were collected with the temperature set at 301 K and the frequency set at 400 MHz. As the solvent, DMSO-d_6 was used when carrying out the NMR spectral studies. The Gouy method was applied to obtain the magnetic data and the $Hg[Co(SCN)_4]$ was employed as reference material. A Thermo-Scientific conductivity meter was used to determine the molecular conductivity.

Synthesis of Schiff base HPPH*m*CB ligand: The pyrrolopyrimidinehydrazide and 3-chlorobenzaldehyde were subjected to reflux for 2 h in absolute ethanol yielding a white solid Schiff base ligand in the solvent. However, upon slow evaporation of solvent at room temperature, a light brown solid product was obtained (**Scheme-I**). The solid material was washed thoroughly with diethyl ether and then recrystallized with ethanol. IR (KBr, ν_{max}, cm^{-1}): 3374 (arom. (N–H)), 3184 (aliph. (N–H)), 2792 (-CH=), 1589 (>C=N), 855 (C-Cl) and 740 (disub. benzene ring). ^{1}H NMR (DMSO-d_6) δ ppm: 13.01 (s, 1H, NH, aromatic), 8.59 (s, 1H, NH, aliphatic), 7.28-8.50 (5H, Ar-H (7.28 (1H, *d, J* = 3.84 Hz), 7.57 (1H, *ddd*, *J* = 8.12, 1.59, 1.28 Hz), 7.59 (1H, *ddd*, *J* = 8.03, 1.55, 1.28 Hz), 7.61 (1H, *td*, *J* = 8.03, 0.51 Hz), 8.075 (2H, *td*, *J* = 1.57, 0.52 Hz), 8.50 (1H, *d, J* = 3.83 Hz). ^{13}C NMR (DMSO-d_6) δ ppm: 139.5 (-CH=), 99.5, 102.3, 126.1, 150.4, 152.54, 163.3 (pyrimidine-C), 120.6, 127.0, 128.73 (aldehydic-C). UV spectrum (λ, nm): 230, 285 ($\pi\rightarrow\pi^*$), 410 ($n\rightarrow\pi^*$).

Synthesis of metal(II) complexes: Following the dissolution of 1.0 mmol of Schff base HPPH*m*CB ligand in 20 mL of methanol, corresponding metal(II) salts (0.50 mmol) were introduced into the solution while stirring and then refluxed for 2 h. The obtained precipitate was filtered, washed with cold methanol and diethyl ether and finally dried in vacuum desiccator. The physico-chemical parameter of the synthesized Schiff base and its metal(II) complexes are complied in Table-1.

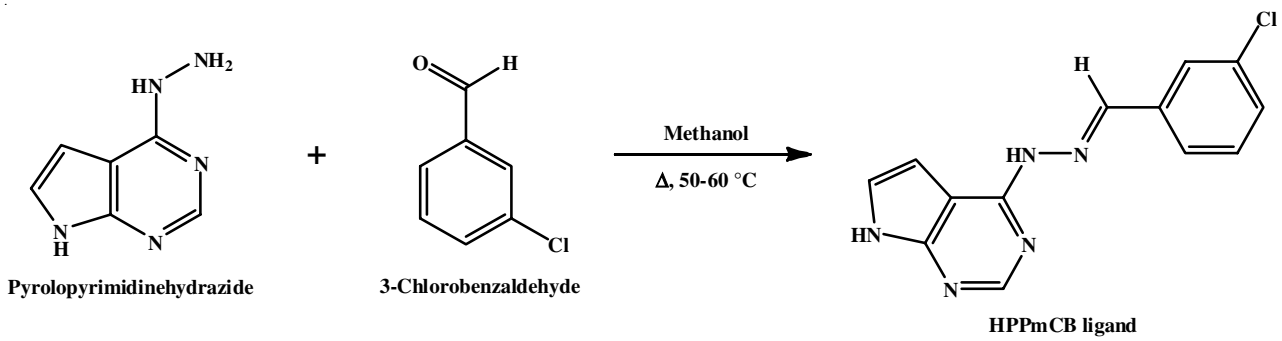

Pyrolopyrimidinehydrazide + **3-Chlorobenzaldehyde** → **HPPmCB ligand**

Scheme-I: Synthetic pathway of HPPH*m*CB ligand

TABLE-1
HPPH*m*CB LIGAND AND METAL(II) COMPLEXES PHYSICO-CHEMICAL AND ANALYTICAL DATA

Compd.	Colour	m.w.	m.f.	Yield (%)	m.p. (°C)	Element analysis (%): Expected (Found)					Conductivity (Ω^{-1} mol^2 cm^{-1})	Magnetic moment (B.M)
						M	C	H	N	Cl		
HPPH*m*CB	Light brown	271.000	$C_{13}H_{10}N_5Cl$	84.61	189	–	57.49 (57.13)	3.71 (3.69)	25.78 (25.73)	13.05 (13.04)	–	–
$Mn(PPHmCB)_2$	White	594.938	$C_{26}H_{18}N_{10}Cl_2Mn$	79.56	228	9.23	52.44 (52.31)	3.03 (3.00)	23.53 (23.53)	11.93 (11.90)	1.570	5.17
$Fe(PPHmCB)_2$	Blue	595.845	$C_{26}H_{18}N_{10}Cl_2Fe$	85.46	238	9.37	52.36 (52.40)	3.02 (3.01)	23.5 (23.44)	11.91 (11.88)	2.983	5.11
$Co(PPHmCB)_2$	Brown	598.993	$C_{26}H_{18}N_{10}Cl_2Co$	83.90	244	9.85	52.09 (52.00)	3.01 (2.99)	23.37 (23.34)	11.90 (11.83)	1.573	4.55
$Ni(PPHmCB)_2$	Green	598.693	$C_{26}H_{18}N_{10}Cl_2Ni$	80.99	258	9.80	52.11 (52.02)	3.01 (3.79)	23.38 (23.36)	11.90 (11.86)	1.946	3.29
$Pd(PPHmCB)_2$	Brown	646.000	$C_{26}H_{18}N_{10}Cl_2Pd$	86.78	245	16.41	48.30 (48.26)	2.79 (2.73)	21.67 (21.53)	7.00 (6.90)	2.658	–
$Cu(PPHmCB)_2$	Green	603.000	$C_{26}H_{18}N_{10}Cl_2Cu$	82.44	238	10.5	51.69 (51.66)	2.98 (2.95)	23.2 (23.19)	11.80 (11.88)	1.868	2.04
$Zn(PPHmCB)_2$	Colourless	605.400	$C_{26}H_{18}N_{10}Cl_2Zn$	80.97	251	10.8	51.54 (51.49)	2.97 (2.93)	23.13 (23.06)	11.70 (11.68)	4.267	–
$Cd(PPHmCB)_2$	Colourless	653.800	$C_{26}H_{18}N_{10}Cl_2Cd$	77.30	256	21.42	47.76 (47.72)	2.77 (2.74)	17.19 (17.11)	10.85 (10.84)	1.028	–
$Hg(PPHmCB)_2$	Colourless	740.590	$C_{26}H_{18}N_{10}Cl_2Hg$	76.78	263	27.09	42.13 (42.11)	2.43 (2.37)	18.9 (18.88)	9.59 (9.55)	0.759	–

[Mn(PPH*m*CB)$_2$]: IR (KBr, ν_{max}, cm^{-1}): 3191 (aliph. N–H), 2980 (-CH=), 1575 (>C=N), 917 (C-Cl), 783 (disub benzene ring), 604 (Mn-N) and 519 (N→Mn). UV spectrum (λ, nm): 425 ($^6A_{1g}\rightarrow{}^4E_g$ (^4D)), 519 (($^6A_{1g}\rightarrow{}^4T_{1g}$ (^4P)).

[Fe(PPH*m*CB)$_2$]: IR (KBr, ν_{max}, cm^{-1}): 3194 (aliph. N–H), 2774 (-CH=), 1574 (>C=N), 844 (C-Cl), 728 (disub. benzene ring), 585 (N-Fe) and 522/504 (N→Fe). UV spectrum (λ, nm): 675 ($^5T_{2g}\rightarrow{}^5E_g$), 435, 415, 240 (LMCT).

[Co(PPH*m*CB)$_2$]: IR (KBr, ν_{max}, cm^{-1}): 3352 (aliph. N–H), 2974 (-CH=), 1549 (>C=N), 875 (C-Cl), 725 (disub. benzene ring), 578 (N-Co) and 516 (N→Co). UV spectrum (λ, nm): 900 ($^4T_{1g}(F)\rightarrow{}^4T_{2g}(F)$), 540 ($^4T_{1g}(F)\,{}^4T_{2g}(P)$).

[Ni(PPH*m*CB)$_2$]: IR (KBr, ν_{max}, cm^{-1}): 3190 (aliph. N–H), 2975 (-CH=), 1587 (>C=N), 888 (C-Cl), 737 (disub. benzene ring), 641 (N-Ni) and 601 (N→Ni). UV spectrum (λ, nm): 971 ($^3A_{2g}$(F)→$^3T_{2g}$(F)), 605 ($^3A_{2g}(F)\,{}^3T_{1g}(F)$).

[Pd(PPH*m*CB)$_2$]: IR (KBr, ν_{max}, cm^{-1}): 3360 (aliph. N–H), 2974 (-CH=), 1588 (>C=N), 875 (C-Cl), 725 (disub. benzene ring), 605 (Pd-N) and 515 (N→Pd). UV spectrum (λ, nm): 445, 377, 301 (LMCT), ^{1}H NMR (DMSO-d_6) δ ppm: 8.688 (s, 2H, -CH= aldehydic), 8.590 (s, 2H, NH, aliphatic), 7.530-8.230 (m, 10H, Ar-H).

[Cu(PPH*m*CB)$_2$]: IR (KBr, ν_{max}, cm^{-1}): 3191 (aliph. N–H), 2977 (-CH=), 1573 (>C=N), 881 (C-Cl), 726 (disub. benzene ring), 604 (Cu-N group) and 520 (N→Cu). UV spectrum (λ, nm): 651 ($^2B_{1g}\rightarrow{}^2A_{1g}$).

[Zn(PPH*m*CB)$_2$]: IR (KBr, ν_{max}, cm^{-1}): 3295 (aliph. N-H), 3076 (-CH=), 1584 (>C=N), 781 (C-Cl), 781 (disub. benzene ring), 643 (Zn-N group) and 593 (N→Zn group). UV spectrum (λ, nm): 410, 356, 221 (LMCT).

[Cd(PPH*m*CB)$_2$]: IR (KBr, ν_{max}, cm^{-1}): 3295 (aliph. N-H), 2974 (-CH=), 1584 (>C=N), 818 (C-Cl), 718 (disub. benzene ring), 582 (Cd-N) and 518 (N→Cd). UV spectrum (λ, nm): 440, 363, 228 (LMCT).

[Hg(PPH*m*CB)$_2$]: IR (KBr, ν_{max}, cm^{-1}): 3193 (aliph. N-H), 2976 (-CH=), 1574 (>C=N), 856 (C-Cl), 725 (disub. benzene ring), 555 (Hg-N) and 519 (N→Hg). UV spectrum (λ, nm): 415, 370, 229 (LMCT).

Antimicrobial assay

Antibacterial activity: The bacterial strains were procured from Microbial Culture Collection (MCC) Pune, India. The Muller Hilton agar medium was subjected to an autoclaving process that lasted for 15 min and conducted at a pressure of 10 Lbs per square inch. Each microbial strain was cultured by swabbing 20 mL of Muller-Hilton agar medium into a Petri dish and then waited for 15 min in order to absorb the culture before continuing the cultivation process. After using a sterile borer to drill the wells, which measured 6 mm in diameter, following the reconstitution of the solutions of each chemical in DMSO, 100 µL of each solution was applied to plates. Over the course of a full day, the temperature of the containers was kept at 37 °C. Calculating each compound's zone of inhibition within the wells served as the basis for determining the antibacterial efficacy of each substance. A positive control was used as a streptomycin and DMSO as a negative control. The method was carried out three times.

Antifungal activity: In cup-plate method, fungi *C. albican* and *S. cerevisiae* were utilized as test subjects for the synthesized compounds. After the test solution was pipetted into discs with a thickness of 1 mm and a diameter of 5 mm, the plates were kept at 37 ºC for 72 h. The diameter of the inhibitor was measured after it had been incubated for 36 h at 37 ºC. Experiments determining the minimum inhibitory concentration were carried out on substances exhibiting potentially antifungal activity. The minimal inhibitory concentration (MIC) of the microbial growth during overnight incubation were measured.

Cytotoxic studies: In a shallow rectangular plastic plate measuring 22 cm × 32 cm, eggs of the brine shrimp (*Artemia salina* Leach) were incubated in an artificial seawater solution prepared from the commercial salt mixture and double-distilled water. A tool with perforations was utilized to separate the plastic dish into its two parts. While the more minor part exposed to natural light was left open, the darker, larger chamber held approximately 50 mg of eggs. After another 2 days, nauplii were pipetted from the lighted side of the dish. The sample was prepared by dissolving 20 mg of test chemical into 2 mL of DMF. Nine vials were filled from stock solutions of 500, 50 and 5 mg/mL (three replicates of each dilution were used for each test sample and the LD_{50} is the mean of three results) and one vial was kept as a control containing 2 mL of DMF. The LD_{50} was determined by taking the average of the three results. The solvent was allowed to evaporate during the night, after 2 days, the shrimp larvae were prepared to be introduced to the saltwater (1 mL in each vial), along with ten adult shrimp and 30 shrimp for each dilution. After that, the volume of each vial was brought up to 5 mL by adding saltwater. After 24 h, a final count of those who had survived was performed [18,19]. The LD_{50} values were determined by applying the Finney computer tool's analysis to the data gathered [20].

RESULTS AND DISCUSSION

Condensation of pyrrolopyrimidinehydrazide and 3-chlorobenzaldehyde yields a novel Schiff base pyrrolopyrimidinehydrazide-*m*-chlorobenzaldehyde (HPPHmCB), which was further used in the preparation of several metal (II) complexes having general formual of [M(PPH*m*CB)$_2$], where M = Mn^{2+}, Cu^{2+}, Fe^{2+}, Co^{2+}, Ni^{2+}, Cd^{2+}, Zn^{2+} and Pd^{2+}. In most of the common organic solvents, all the synthesized compounds are found to be soluble.

FT-IR spectral studies: Upon deprotonation, the aromatic imine group (–NH) contributes to bonding, as evidenced by the band's disappearance at 3374 cm^{-1} in the ligand's IR spectrum [21], which was also absent in the IR spectra of the metal (II) complexes. After the metal complexation, the azome-thine C=N stretching vibration of the Schiff base HPPH*m*CB ligand shifted from 1589 to 1573-1584 cm^{-1}. The reason is attributed due to the deprotonation occurring during the complexation process. The Schiff base ligand showed an aromatic C=N stretching band at 1648-1642 cm^{-1}, however, a slight shift in the vibrational stretch of 13-25 cm^{-1} was observed upon complexation (Fig. 1) [22,23]. Moreover, the bands at 641-578 and 601-507 cm^{-1} were observed in the spectra of the metal(II) complexes, which may originate from ν(N-M) and ν(N→M) stretches.

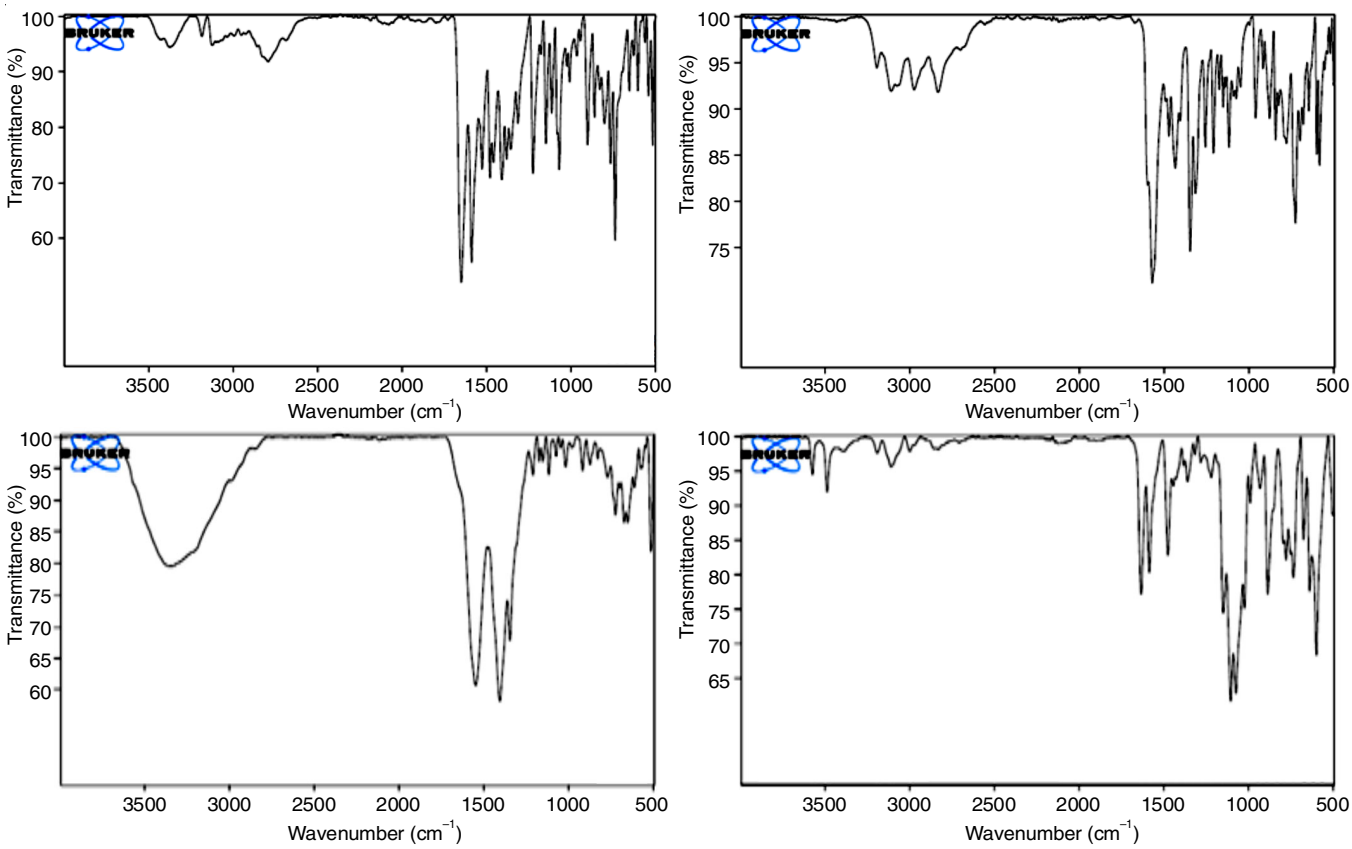

Fig. 1. The ligand and its metal complex FT(IR) spectrum

^{1}H NMR spectral studies: The Pd(II) complex was further characterized by ^{1}H NMR spectra using DMSO-d_6 as solvent. The Pd(II) complex ^{1}H NMR spectrum showed the identical peaks to those in free HPPH*m*CB ligand of ^{1}H NMR spectrum. The aromatic amine that serves as ligand for HPPH*m*CB exhibited a signal at 13.01 ppm, whereas the ^{1}H NMR spectrum of Pd(II) complex was devoid of this NH signal. Consequently, coordination occurred using the deprotonated aromatic NH group during the complexation process. The aromatic (NH) was detected for the Pd(II) complex at δ 8.59 ppm (s, 1H, NH), which was in agreement with the standard literature. The proton of pyrimidine ring exhibited distinct signal at δ 8.49 ppm, whereas protons of aromatic rings (Ar-H) signaled between 7.53-8.18 ppm.

UV-Vis spectral and magnetic moment measurements: Complexes of elements Fe(II), Co(II), Ni(II), Mn(II) and Cu(II) synthesized exhibited magnetic moments of 5.11, 4.55, 3.29, 5.17 and 2.04 B.M., respectively (Table-1). By measuring magnetic susceptibilities, the octahedral structures were verified for Fe(II), Co(II), Ni(II), Mn(II) and Cu(II) complexes [24,25]. The diamagnetic property confirmed the square planar structure of Pd(II) and the tetrahedral geometry of Hg(II), Zn(II) and Cd(II) complexes.

The UV-Vis spectrum of novel HPPH*m*CB ligand and its metal(II) complex in DMF were recorded between 190-1000 nm. The n→π* and π→π* transitions in the pyrrole, pyrimidine and imine groups were attributed to bands at 410, 285 and 230 nm in the HPPH*m*CB ligand spectrum. All the metal(II) complexes all showed n→π* and π→π* transitions between 375 and 249 nm, corresponding to the azomethine, pyrrole and pyrimidine ring transitions.

The magnetic susceptibility measurement data revealed that [Fe(PPH*m*CB)$_2$] complex is paramagnetic at 301 K, indicating its iron oxidation state of +2. The absorption band at 675 nm in the electronic spectra of the Fe(II) complex was ascribed to $^5T_{2g}\rightarrow{}^5E_g$ transition [26]. The L→M charge transfer band was found to be at 435, 415 and 240 nm. The [Fe(PPH*m*CB)$_2$] complex exhibited magnetic moment of 5.11 B.M., as predicted by high spin octahedral geometry [27,28]. Absorptions at 900 and 540 nm for the [Co(PPH*m*CB)$_2$] complex suggest an octahedral geometry surrounding the Co(II) ion [29]. These absorptions were ascribed to the $^4T_{1g}(F)\rightarrow{}^4T_{2g}(F)$ (ν_1) and $^4T_{1g}(F)\rightarrow{}^4T_{2g}(P)$ (ν_1) transitions, respectively. The computed value of ν_3 was found tobe closer to the charge transfer transition between metal and ligand [30,31].

Two bands, at 971 and 605 nm, were observed in the electronic spectra of the Ni(II) complex. These bands were assigned to the $^3A_{2g}(F)\rightarrow{}^3T_{2g}(F)$ (1) and $^3A_{2g}(F)\rightarrow{}^3T_{1g}(F)$ (ν_2) transitions, respectively [32]. Band at 651 nm for copper complex of the HPPH*m*CB ligand was ascribed to the $^2B_{1g}\rightarrow{}^2A_{1g}$ (ν_1) transition. It has a square planar shape, forming a distinctive band around Cu(II) [33]. For octahedral complexe [34], the magnetic moment value of 2.04 B.M. at room temperature was within the limit. Small absorption bands at 425 and 519 nm in the electronic spectra of the homo-binuclear [Mn(PPH*m*CB)$_2$] complex were assigned as $^6A_{1g}\rightarrow{}^4E_g(4D)$ and $^6A_{1g}\rightarrow{}^4T_{1g}(4P)$, respectively

TABLE-2
ANTIMICROBIAL ACTIVITY DATA OF THE SCHIFF BASE HPPH*m*CB LIGAND AND ITS METAL(II) COMPLEXES

Compound	Antibacterial activity				Antifungal activity	
	B. subtilis	*P. aeruginosa*	*E. coli*	*S. aureus*	*C. albicans*	*S. cerevisiae*
HPPH*m*CB	6	7	7	6	20	6
Fe(II)	8	8	7	6	21	9
Co(II)	7	8	7	7	18	8
Ni(II)	11	9	12	13	12	12
Pd(II)	8	8	11	6	18	8
Cu(II)	8	7	7	6	11	9
Mn(II)	7	7	8	10	6	10
Zn(II)	9	9	8	6	9	11
Cd(II)	11	9	7	8	10	9
Hg(II)	6	7	7	6	13	8

[35]. This was consistent with octahedral geometry of metal(II) complexes. In case of [Mn(PPH*m*CB)$_2$] complex, the high spin octahedral form was further supported by measured magnetic moment value of 5.17 B.M. [36,37]. The UV spectra of Pd(II), Hg(II), Cd(II) and Zn(II) complexes exhibited strong bands at 410-445, 356-377 and 221-301 nm, respectively attributed to intra-ligands and LMCT transitions. These spectral lines points to a nitrogen-atom link between HPPH*m*CB and metal(II) at positions [38,39].

ESR spectral studies: The ESR spectra of [Cu(PPH*m*CB)$_2$] is indicative of species with d^9 configuration and an axial symmetry type of $d_{x^2-y^2}$ ground state [40]. The tetragonal deformation [41] and elongation along fold symmetry *z*-axis, the value of g_{iso} having 2.13 and 2.07 indicated the isotropic type. The relation between g-values is denoted as G and is expressed as per the formula given in eqn 1:

$$G = \frac{g_{\parallel} - 2}{g - 2} \quad (1)$$

If G value of complex is greater than 4.0, it indicates local tetragonal axes are parallel or slightly asymmetrical. If G is equal or less than 4.0 it indicates significant exchange coupling. Whereas if complex has a G value lower than 4.0, it indicates presence of tetragonal axes in structure. Surprisingly, the g values for these complexes were lower than 2.3, which indicate that copper(II) ion was surrounded by a large number of covalent bonds [41,42]. Additionally, the covalence parameter in the plane is denoted by α^2(Cu). This fact is supported by computed values of 0.75, which indicates that [Cu(PPH*m*CB)$_2$] complex possesses covalent bond nature [43]. The ratio of $g_{\parallel}/A_{\parallel}$ can be used to deduce the stereochemistry of copper(II) complex. According to the hypothesis presented by Karlin *et al*. [44], this ratio may provide some insight into the stereochemistry of copper(II) complex. Copper(II) complexes have a square planar geometry, which is conformed from the $g_{\parallel}/A_{\parallel}$ quotient value in the range of 163-170 cm^{-1}, whereas the tetragonally deformed complexes are predicted to have a value which is larger than 144 cm^{-1}. The tentative structures of the synthesized metal(II) complexes are shown in Fig. 2.

Biological studies

Antibacterial studies: As per the results of antibacterial study, the synthesized metal(II) complexes were found to exhibit inhibition zone ranging from 6 mm to 13 mm against *S. aureus*, *B. subtilis*, *E. coli* and *P. aeruginosa* in a screening experiment. The metal(II) complexes inhibitory values ranged from 7 to 13 mm, which rendered them more potent against *S. aureus* than the Schiff base HPPH*m*CB ligand. Increased lipophilicity, as according to chelation theory [45], allowed easier translocation through lipid bilayers of bacterial membranes. By exchanging some of the metal charge for that of ligands donor groups, reduced the polarity of metal(II) atom. The Ni(II) complex showed greater zone of inhibition than any other compound or reference medication streptomycin, which was 12 mm. The higher value of Hg(II) complex can be attributed to coordination of Hg^{2+} ions with ligands, which rendered complex to be more bioactive and dangerous by facilitating the penetration of cell-lipid barrier and impeding and destroying the respiration process of test organism [46,47]. The Hg(II) complex exhibited inhibitory zone of 10, 9, 12 and 13 mm against *S. aureus*, *B. subtilis*, *E. coli* and *P. aeruginosa*, whereas streptomycin had inhibitory zones of 10, 10, 12 and 14 mm.

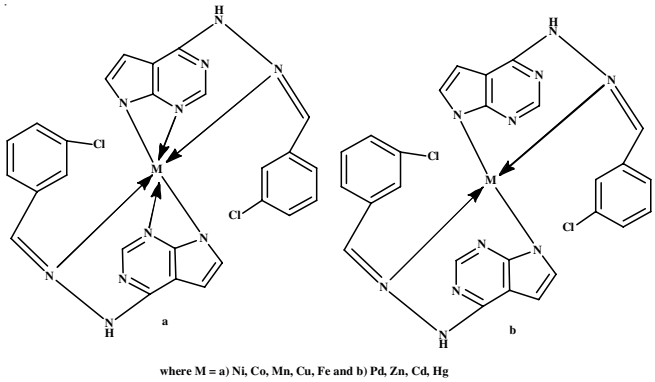

Fig. 2. Tentative structure of metal(II) complexes having tridentate Schiff base derived from pyrrolopyrimidine

Antifungal studies: Based on the results of antifungal study, it was revealed that the Schiff base HPPH*m*CB ligand and its metal(II) complexes exhibited around 2.5 times the potency of fluconazole against *C. albicans* (12-21 mm), except Mn(II) complex, whose zone of inhibition against *C. albicans* (6 mm) was close to fluconazole (11 mm). Study also revealed that *S. cerevisiae* and *C. albicans* were unable to dissolve the transition chemicals (Table-2).

Cytotoxic bioassay: The cytotoxicity study (Brine shrimp bioassay) of metal(II) complexes was done as per the standard protocol of Meyer *et al*. [19]. The results (Table-3) shows that

TABLE-3
CYTOTOXIC BIOASSAY OF HPPH*m*CB
LIGAND AND ITS METAL(II) COMPLEXES

Compound	LD_{50} (µg/mL)	Compound	LD_{50} (µg/mL)
HPPH*m*CB	150	$Cu(PPHmCB)_2$	125
$Fe(PPHmCB)_2$	125	$Zn(PPHmCB)_2$	100
$Co(PPHmCB)_2$	125	$Cd(PPHmCB)_2$	80
$Ni(PPHmCB)_2$	100	$Hg(PPHmCB)_2$	75
$Pd(PPHmCB)_2$	90	$Mn(PPHmCB)_2$	125

only three complexes *viz*. Pd(II), Mn(II) and Hg(II) displayed considerable cytotoxic effects against *Artemia salina*. The Hg(II) complex showed the highest activity (LD_{50} = 75 µg/mL) in this series, whereas the Schiff base HPPH*m*CB ligand had the lowest (LD_{50} = 150 µg/mL), which revealed that coordination makes the lessen the complex' cytotoxicity.

Conclusion

Present study involved the synthesis, characterization and biologcial activity of few transition metal(II) complexes with tridentate Schiff base derived from pyrrolopyrimidine. The results suggested that metal(II) complexes (M = Cu^{2+}, Fe^{2+}, Ni^{2+}, Mn^{2+} & Co^{2+}) have octahedral structure, whereas Cd^{2+}, Zn^{2+} & Hg^{2+} complexes exhibited tetrahedral shape, but atlast, Pd^{2+} complex has a square planar structure. Chelation of metals with organic ligand improved the synergy of all synthetic metal complexes, which led to exceptional effectiveness against bacteria. This coordinated effort has increased the potential for the synthetic metal(II) complexes to be developed into antimicrobial lead candidates by increasing their efficiency in inhibiting *P. aeruginosa*, *B. subtilis*, *S. aureus* and *E. coli*.

CONFLICT OF INTEREST

The authors declare that there is no conflict of interests regarding the publication of this article.

REFERENCES

1. R. Herna'ndez-Molina and A. Mederos, in Comprehensive Coordination Chemistry II, vol. 1, ed. by J.A. McCleverty, T.J. Meyer (Elsevier, Amsterdam, 2004), p. 411.
2. M. Andruh and F. Tuna, in Focus on Organometallic Chemistry Research, ed. by M.A. Cato (Nova Publishers, Hauppauge, 2005), p. 144.
3. A.J. Atkins, D. Black, A.J. Blake, A. Marin-Becerra, S. Parsons, L. Ruiz-Ramirez and M. Schröder, *Chem. Commun. (Camb.)*, **4**, 457 (1996); https://doi.org/10.1039/CC9960000457
4. P.A. Vigato and S. Tamburini, *Coord. Chem. Rev.*, **248**, 1717 (2004); https://doi.org/10.1016/j.cct.2003.09.003
5. P.A. Vigato, S. Tamburini and L. Bertolo, *Coord. Chem. Rev.*, **251**, 1311 (2007); https://doi.org/10.1016/j.ccr.2006.11.016
6. M. Sakamoto, K. Maneski and H. Okawa, *Coord. Chem. Rev.*, **219–221**, 379 (2001); https://doi.org/10.1016/S0010-8545(01)00341-1
7. G. Ceyhan, C. Celik, S. Urus, I. Demirtas, M. Elmastas and M. Tu¨mer, *Spectrochim. Acta A Mol. Biomol. Spectrosc.*, **81**, 184 (2011); https://doi.org/10.1016/j.saa.2011.05.106
8. R. Herchel, I. Nemec, M. Machata and Z. Trávníèek, *Inorg. Chem.*, **54**, 8625 (2015); https://doi.org/10.1021/acs.inorgchem.5b01271
9. N.S. Youssef, E.A. El-Zahany and M.A. El-Seidy, *Phosphorus Sulfur Silicon Relat. Elem.*, **185**, 785 (2010); https://doi.org/10.1080/10426500902967904
10. N.K. Chaudhary and P. Mishra, *Bioinorg. Chem. Appl.*, **2017**, 1 (2017); https://doi.org/10.1155/2017/6927675
11. W.A. Zoubi, A.A.S. Al-Hamdani and Y.G. Ko, *J. Sep. Sci. Technol.*, **52**, 1052 (2017); https://doi.org/10.1080/01496395.2016.1267756
12. X. Liu and J.-R. Hamon, *Coord. Chem. Rev.*, **389**, 94 (2019); https://doi.org/10.1016/j.ccr.2019.03.010
13. H.L. Singh, S. Khaturia, V.S. Solanki and N. Sharma, *J. Indian Chem. Soc.*, **100**, 100945 (2023); https://doi.org/10.1016/j.jics.2023.100945
14. U. Spichiger-Kelle, Chemical Sensors and Biosensors for Medical and Biological Applications (Wiley, Weinheim, 1998).
15. R. Stock and B.F.R. Cedric, *Chromatographic methods*. Springer, 2013.
16. Y.M. Ahmed, W.H. Mahmoud, M.M. Omar and G.G. Mohamed, *J. Inorg. Organomet. Polym. Mater.*, **31**, 2339 (2021); https://doi.org/10.1007/s10904-020-01867-1
17. S. Kula, P. Ledwon, A.M. Maroñ, M. Siwy, J. Grzelak, M. Szalkowski, S. Mackowski and E. Schab-Balcerzak, *Dyes Pigments*, **192**, 109437 (2021); https://doi.org/10.1016/j.dyepig.2021.109437
18. A.S. Abu-Khadra, R.S. Farag and A.E.D.M. Abdel-Hady, *Am. J. Anal. Chem.*, **7**, 233 (2016); https://doi.org/10.4236/ajac.2016.73020
19. B.N. Meyer, N.R. Ferrigni, J.E. Putnam, L.B. Jacobsen, D.E.J. Nichols and J.L. McLaughlin, *Planta Med.*, **45**, 31 (1982); https://doi.org/10.1055/s-2007-971236
20. R.M. Russell and J.L. Robertson, *Bulletin of the ESA*, **25**, 191 (1979).
21. A. Gencer Imer, R.H. Syan, M. Gülcan, Y.S. Ocak and A. Tombak, *J. Mater. Sci. Mater. Electron.*, **29**, 898 (2018); https://doi.org/10.1007/s10854-017-7986-z
22. V.P. Singh, S. Singh, D.P. Singh, K. Tiwari and M. Mishra, *J. Mol. Struct.*, **1058**, 71 (2014); https://doi.org/10.1016/j.molstruc.2013.10.046
23. W. Hernández, J. Paz, F. Carrasco, A. Vaisberg, E. Spodine, J. Manzur, L. Hennig, J. Sieler, S. Blaurock and L. Beyer, *Bioinorg. Chem. Appl.*, **2013**, 524701 (2013); https://doi.org/10.1155/2013/524701
24. M. So¨nmez, M. Celebi, A. Levent, I. Berber, Z. Senturk, *J. Coord. Chem.*, **63**, 848 (2010).
25. S. Ilhan, H.M. Baykara, S. Seyitoglu, A. Levent, S. Özdemir, A. Dündar, A. Öztomsuk and M.H. Cornejo, *J. Mol. Struct.*, **1075**, 32 (2014); https://doi.org/10.1016/j.molstruc.2014.06.062
26. B.E. Van Kuiken, A.W. Hahn, B. Nayyar, C.E. Schiewer, S.C. Lee, F. Meyer, T. Weyhermüller, A. Nicolaou, Y.-T. Cui, J. Miyawaki, Y. Harada and S. DeBeer, *Inorg. Chem.*, **57**, 7355 (2018); https://doi.org/10.1021/acs.inorgchem.8b01010
27. M. Tarrago, C. Römelt, J. Nehrkorn, A. Schnegg, F. Neese, E. Bill and S. Ye, *Inorg. Chem.*, **60**, 4966 (2021); https://doi.org/10.1021/acs.inorgchem.1c00031
28. R.R. Badekar, S.W. Kulkarni, R.S. Lokhande and B.S. Thawkar, *Int. J. Appl. Res.*, **2**, 175 (2016).
29. M.A. Al-Omair, *Arab. J. Chem.*, (2018); https://doi.org/10.1016/j.arabjc.2018.11.006
30. M. Orojloo, P. Zolgharnein, M. Solimannejad and S. Amani, *Inorg. Chim. Acta*, **467**, 227 (2017); https://doi.org/10.1016/j.ica.2017.08.016
31. S.M. Emam, S.A. AbouelEnein and E.M. AbdelSatar, *Appl. Organomet. Chem.*, **33**, e4847 (2019); https://doi.org/10.1002/aoc.4847
32. I. Ali, W.A. Wani, A. Khan, A. Haque, A. Ahmad, K. Saleem and N. Manzoor, *Microb. Pathog.*, **53**, 66 (2012); https://doi.org/10.1016/j.micpath.2012.04.005
33. C.A. Téllez S, A.C. Costa Jr., M.A. Mondragón, G.B. Ferreira, O. Versiane, J.L. Rangel, G.M. Lima and A.A. Martin, *Spectrochim. Acta A Mol. Biomol. Spectrosc.*, **169**, 95 (2016); https://doi.org/10.1016/j.saa.2016.06.018
34. S.P. Sellers, B.J. Korte, J.P. Fitzgerald, W.M. Reiff and G.T. Yee, *J. Am. Chem. Soc.*, **120**, 4662 (1998); https://doi.org/10.1021/ja973787a
35. L.H. Abdel-Rahman, A.M. Abu-Dief, R.M. El-Khatib, S.M. Abdel-Fatah and A.A. Seleem, *Int. J. Nano. Chem.*, **2**, 83 (2016); https://doi.org/10.18576/ijnc/020303

36. H. Sakiyama, M. Kato, S. Sasaki, M. Tasaki, E. Asato and M. Koikawa, *Polyhedron*, **111**, 32 (2016); https://doi.org/10.1016/j.poly.2016.03.005
37. H. Masai, K. Sonogashira and N. Hagihara, *Bull. Chem. Soc. Jpn.*, **44**, 2226 (1971); https://doi.org/10.1246/bcsj.44.2226
38. K. Peng, V. Mawamba, E. Schulz, M. Löhr, C. Hagemann and U. Schatzschneider, *Inorg. Chem.*, **58**, 11508 (2019); https://doi.org/10.1021/acs.inorgchem.9b01304
39. V. Vindya, V. Sadasivan, S.S. Meena and P. Bhatt, *Orient. J. Chem.*, **34**, 45 (2018); https://doi.org/10.13005/ojc/340105
40. R. Èerný, N. Penin, H. Hagemann and Y. Filinchuk, *J. Phys. Chem. C*, **113**, 9003 (2009); https://doi.org/10.1021/jp9015883
41. Y. Sindhu, C.J. Athira, M.S. Sujamol, R.S. Joseyphus and K. Mohanan, *Synth. React. Inorg. Met.-Org. Nano-Met. Chem.*, **43**, 226 (2013); https://doi.org/10.1080/15533174.2012.740711
42. M.S. Suresh and V. Prakash, *E-J. Chem.*, **8**, 1408 (2011); https://doi.org/10.1155/2011/254018
43. M. Stylianou, C. Drouza, Z. Viskadourakis, J. Giapintzakis and A.D. Keramidas, *Dalton Trans.*, 6188 (2008); https://doi.org/10.1039/b803854f
44. K.D. Karlin, J.C. Hayes, S. Juen, J.P. Hutchinson and J. Zubieta, *Inorg. Chem.*, **21**, 4106 (1982); https://doi.org/10.1021/ic00141a049
45. M.S.S. Adam, H. Elsawy, A. Sedky and M.M. Makhlouf, *J. Taiwan Inst. Chem. Eng.*, **136**, 104425 (2022); https://doi.org/10.1016/j.jtice.2022.104425
46. L. Buzón-Durán, R. Capita and C. Alonso-Calleja, *Food Microbiol.*, **72**, 220 (2018); https://doi.org/10.1016/j.fm.2017.11.018
47. S. Le Page, D. Raoult and J.M. Rolain, *Int. J. Antimicrob. Agents*, **45**, 61 (2015); https://doi.org/10.1016/j.ijantimicag.2014.08.014